Proceedings of the Sixteenth (2006) International Offshore and Polar Engineering Conference
San Francisco, California, USA, May 28-June 2, 2006

ISBN 1-880653-66-4 (Set); ISSN 1098-6189 (Set)

A Nonlinear Model for Oscillating Water Column Analysis, Design and Control

G.D. Gkikas, N.I. Xiros, G.A. Athanassoulis and K. A. Belibassakis
School of Naval Architecture and Marine Engineering, National Technical University of Athens.
Athens, GREECE

ABSTRACT

A model for the energy exchanges involved in OWC power-plants is proposed. The model is using data series generated by numerical codes developed on the basis of relative physical principles. The ocean wave field and the oscillating water column are modeled according to linear water wave theory as a waveguide excited at both ends. The thermodynamic process inside the chamber is modeled with a control-volume approach. Then by applying identification techniques for linear and nonlinear systems, the corresponding operator representations are obtained in the frequency domain. A closed-loop is finally constructed which may find use in analysis and synthesis of OWC systems.

KEY WORDS: Oscillating Water Colum, analysis and control.

INTRODUCTION

As pointed by many authors, see, e.g., Thiruvenkatasamy & Neelamani (1997), Falcao (2001), Falcao & Rodrigues (2002), Falcao (2002), and others, the oscillating-water-column (OWC) is probably one of the the most promising devices for the efficient extraction of energy from ocean waves. Also, the present development of OWC has reached the stage of development of full-sized prototypes, requiring the development of accurate methods for OWC analysis and control.

Wave-energy converters of the oscillating-water-column (OWC) type with pneumatic power take-off may be modelled by the so-called method of 'applied-pressure' description. The objective of this work is to develop a model for the dynamics of energy exchanges involved in Oscillating Water Column (OWC) wave energy extraction systems. The proposed model can be used in future studies which aim to improve overall efficiency of the installation. Therefore, it is based on system identification techniques for obtaining representations of the linear and nonlinear operators depicting the action of each physical subsystem. Furthermore, the identification techniques employed and, consequently, the operator representations obtained are in the frequency domain, due to reasons to be more clearly explained later.

The input-output data series required for system identification have been obtained by use of numerical codes, developed on the basis of previous works on the subject. Following the works by Evans (1982) and Evans & Porter (1995), the OWC system is partitioned to a hydrodynamic and a thermodynamic part. The hydrodynamic part consists of the water column inside the OWC chamber (see Fig. 1), as well as the wave field outside of the chamber and offshore. This part is modeled as a waveguide excited at both ends. The offshore end is excited by a far-field, incident waveform, and the in-chamber end is excited by the entrapped air pressure fluctuation with respect to atmospheric pressure. The numerical code is based on linear water wave theory. Corresponding to the double-end excitation of the waveguide, the velocity potential inside the wave field is partitioned to a radiating and a scattering part. Due to the linearity assumption, the two parts of the response may be superimposed at any point within the wave field in order to give the value of any variable of interest e.g. velocity, pressure, wave height etc. Effectively, the hydrodynamic waveguide is modeled as a distributed linear system. On the other hand, the thermodynamic part of the OWC system is modeled as a lumped but nonlinear system, following previous formulations of similar open thermodynamic systems Gyftopoulos & Beretta (1991). Specifically, the equations are originally formulated and solved in the time domain. Then, the frequency response is obtained by imposing single tones at various frequencies and obtaining the response, which is of course multi-chromatic, due to the underlying nonlinearities.

The system identification techniques employed for the two parts, although both in the frequency domain, differ significantly. For the linear, distributed hydrodynamic part a modal decomposition approach is adopted which allows to reduce the degrees of freedom to a finite number. The tradeoff involved here is that the reduced-order model is approximating the dominant dynamics in just a limited frequency band of interest. For the nonlinear, thermodynamic part a Volterra-Wiener approach is adopted which leads to a truncated polynomial representation. The determination of either the Volterra homogeneous kernels or the Wiener G-functionals is performed in a frequency-domain, Least Square Error (MSE) framework. In this work, we are focused on the Volterra homogeneous kernel identification. This is achieved by applying an a priori structure to the nonlinear model of the thermodynamic part and, then, obtaining the response to monochromatic inputs. In a future work, the Wiener G-functionals will be determined by driving the system with white noise forcing. It is noted here that the latter approach is far more general as it reveals the full dynamics and provides with an orthogonal operator expansion that can be used for any deterministic or stochastic excitation signal.

The frequency-domain operator representations, obtained for both the hydrodynamic and thermodynamic subsystems, are incorporated in the closed-loop configuration shown in Fig. 2. At a first glance, this configuration has been inspired by the physical principles governing energy exchange interactions in a typical OWC system. Indeed, as shown in Fig. 1, the in-chamber water column free surface acts as a reciprocating piston for the air mass entrapped in the chamber above it. Therefore, one may consider that the spatial average at any instant of the in-chamber water wave height is the driving signal of the air pressure. The dynamics of this interaction are depicted by the truncated

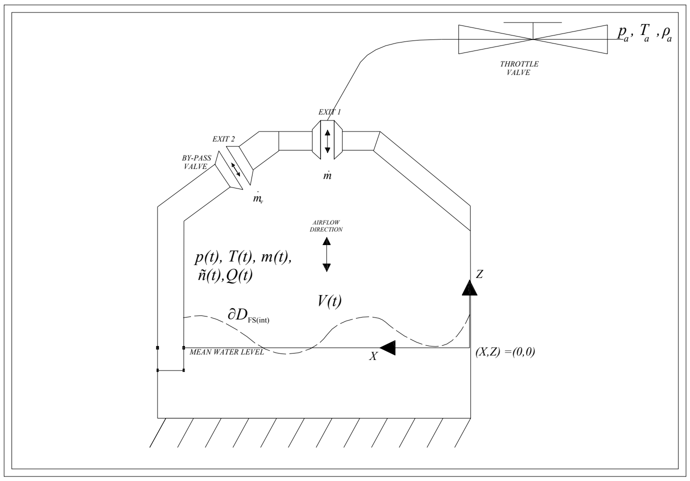

Fig. 1: Schematic presentation of OWC chamber.

polynomial operator of the thermodynamic part. Average spacing is required in order to interface correctly the distributed hydrodynamic subsystem to the lumped thermodynamic one. On the other hand, the water column height is determined by both the far field excitation, through the linear operator of the scattering part and the entrapped air pressure, through the linear operator of the radiating part. The frequency-domain representations of both these operators are obtained by the modal decomposition approach.

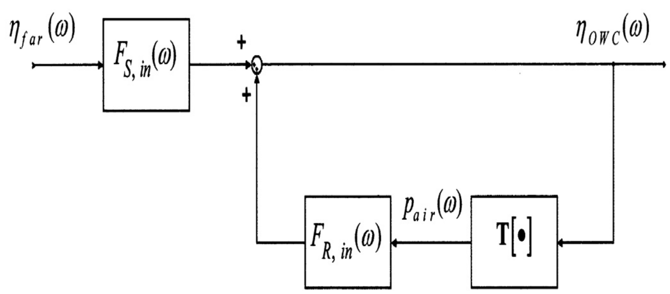

Fig. 2: Closed-loop OWC configuration.

In effect, one may express the wave height $\eta(x,\omega)$ at any point in the wave field as follows:

$$\eta(x,\omega) = F_S(x,\omega)\eta_{far}(\omega) + F_R(x,\omega)p_{air}(\omega)\ , \tag{1}$$

For the entrapped air pressure it holds that:

$$p_{air}(\omega) = \mathbf{T}\left[\eta_{OWC}(\omega)\right],\ \text{where}\ \ \eta_{OWC}(\omega) \triangleq \frac{1}{S_i}\int_{\partial D_i}\eta(x,\omega)dx, \tag{2}$$

and $S_i \triangleq \int_{\partial D_i} dx$. It is evident that:

$$\begin{aligned}\eta_{OWC}(\omega) &= F_{S,in}(\omega)\eta_{far}(\omega) + F_{R,in}(\omega)p_{air}(\omega) = \\ &= F_{S,in}(\omega)\eta_{far}(\omega) + F_{R,in}(\omega)\cdot\mathbf{T}\left[\eta_{OWC}(\omega)\right],\end{aligned} \tag{3}$$

where $F_{S,in}(\omega) \triangleq \frac{1}{S_i}\int_{\partial D_i} F_S(x,\omega)dx, F_{R,in}(\omega) \triangleq \frac{1}{S_i}\int_{\partial D_i} F_R(x,\omega)dx$.

Based on the above we finally obtain:

$$\eta_{OWC}(\omega) = \left\{\mathbf{I} - F_{R,in}\left[\mathbf{T}\right]\right\}^{-1}\left[F_{S,in}(\omega)\eta_{far}(\omega)\right], \tag{4}$$

where **I** denotes the unity operator and the brackets indicate connection of systems (linear or nonlinear) in cascade. The above frequency-domain relation governs the transfer of energy from the far-field excitation $\eta_{far}(\omega)$ to the equivalent piston displacement $\eta_{OWC}(\omega)$ driving the thermal subsystem of the installation.

For analysis of a given OWC installation, i.e. with a priori knowledge of geometrical configuration data of the hydrodynamic waveguide and air chamber, turbine and possible bypass valve characteristics etc., the energy transfer relation is of major importance. Indeed, it allows evaluation of the matching between the plant design and the wave climate at the installation site, specified by the Power Spectral Density (psd) of the wave height signal. Practically, this is equivalent to specifying the psd of $\eta_{far}(\omega)$. Therefore, the operator interconnecting its psd to that of the equivalent piston displacement $\eta_{OWC}(\omega)$ demonstrates the "resonation characteristics" of the energy transfer process, that is whether the OWC plant configuration selected is terminating the hydrodynamic waveguide of the installation site with a power reflection coefficient as small as possible at the frequency band where the far-field psd demonstrates its peaks.

In the case that the above condition is not met satisfactorily, design of either the thermodynamic subsystem or the hydrodynamic waveguide or both needs to be modified in order to achieve improved performance. The design objectives are in general two. One is to place the resonance area of the thermodynamic subsystem around the peaks of the far-field psd, and another is to increase the width of the OWC system's resonance band. In many cases, both these objectives can be met just by passive modification of the physical design, i.e. configuration of the waveguide geometry, re-dimensioning of the chamber, change of the turbine etc. Alternatively, and especially when related costs are high, the introduction of active, feedback control of the plant may prove of significant value. Some of the challenging control problems involved in OWC systems and where the proposed model may prove useful include: selection of the control objectives, measured and control variables; synthesis of the control law and robustness assessment of the controller.

OWC HYDRODYNAMICS

In the framework of linear wave theory (Mei, 1983, Evans and Porter 1995), the total flow behaviour inside and around the OWC can be described by an appropriate superposition of scattering ϕ^S and radiation ϕ^R complex wave potentials. The part $\phi^S = \phi^S(x,z;\omega)$ contains the incident and the scattered wave, associated with a specific incident wave frequency ω, and the part $\phi^R(x,z;\omega)$ models the radiated wave field due to the oscillation of the trapped air inside the chamber of OWC, parametrically dependent on the frequency ω.

For simplicity in the presentation we shall restrict ourselves to the 2D case; see Fig.3. The flow domain D is subdivided into three sub-domains $D = D_1 \bigcup D_2 \bigcup D_3$, as shown in Fig.3, where

$$D_i = \left\{(x,z):\ x_{i+1} < x < x_i,\ -h < z < s_i\right\},\ i=1,2,3,$$

where $s_1 = s_3 = 0$ and $s_2 = -h_1$, and $x_1 = \infty$, $x_2 = \varepsilon$, $x_3 = b$, and $x_4 = 0$.

It is stressed here that, in contrast to the approach by Evans and Porter

(1995), in the present work the hydrodynamic problems are formulated for a finite chamber wall thickness $(\varepsilon - b)$; see Fig. 3.

The complex velocity potentials, ϕ^S and ϕ^R, must satisfy the Laplace equation

$$\nabla^2 \phi^{S,R} = 0 \quad , \quad \text{in each sundomain } D_i,\ i = 1,2,3 \quad , \tag{5}$$

the no-entrance boundary condition on every solid boundary (∂W) of the OWC,

$$\left[\frac{\partial \phi^{S,R}}{\partial n} \right]_{\partial W} = 0 \ , \tag{6}$$

as well as on the horizontal sea bed,

$$\frac{\partial \phi^{S,R}}{\partial z} = 0, \quad \text{on} \quad z = -h \ . \tag{7}$$

Moreover, the following boundary conditions must be satisfied on the upper water surface outside (S_e) and inside (S_i) the OWC, respecively:

$$\frac{\partial \phi^{S,R}}{\partial z} - \frac{\omega^2}{g} \phi^{S,R} = f^{S,R}, \quad \text{on} \quad z = 0 \ , \tag{8}$$

where $f^S = 0$, and $f^S = 0$, for $x > \varepsilon$, and $f^R = 1$, for $x < b$.

Finally, the above formulation is completed by appropriate conditions at infinity, requiring that ϕ^S behaves like the superposition of a plane incident and a reflected wave,

$$\phi^S(x,z) \sim \phi^S_\infty(x,z) = \left(e^{-ik_0(x-\varepsilon)} + A_0^S e^{ik_0(x-\varepsilon)} \right) Z_0^{(1)}(z), \ \text{as} \ x \to \infty \ , \tag{9a}$$

and ϕ^R behaves like an outgoing plane wave.

$$\phi^R(x,z) \sim \phi^S_\infty(x,z) = A_0^R \exp\left(ik_0(x-\varepsilon)\right) Z_0^{(1)}(z), \quad \text{as} \quad x \to \infty \ . \tag{9b}$$

In the above equations $k_0 = k_0^{(1)}$ is the wavenumber associated with the propagating mode, obtained as the positive real root of the dispersion relation, formulated at the (constant) depth h,

$$K = g \tanh(kh), \quad K = \omega^2 / g \quad , \qquad \text{and} \tag{10a}$$

$$Z_0^{(1)}(z) = \cosh\left(k_0^{(1)}(z+h)\right) / \cosh\left(k_0^{(1)} h\right) \ . \tag{10b}$$

In Eqs. (9) $A_0^{S,R}$ denote the complex amplitudes of the scattered and radiated wave field, respectively.

In accordance with the domain decomposition, the wave potentials ϕ^S and ϕ^R will be obtained by formulating complete modal-type representations in each subregion (see, e.g., Mei & Black, 1969, Black et al, 1971, Evans and Porter 1995), and requiring their complete matching at the vertical interfaces separating the three subdomains (matching of the potential and its normal derivative).

<u>Region 1 ($\varepsilon < x$)</u>

The general representations of the velocity potentials $\phi^{S,R}$ in the semi-infinite subdomain D_1 are given by

$$\phi_{(1)}^{S,R}(x,z) = \phi_\infty^{S,R}(x,z) + \sum_{n=1}^{\infty} A_n^{S,R} \exp\left(-k_n^{(1)}(x - \varepsilon)\right) Z_n^{(1)}(z) \quad , \tag{11}$$

where $\phi_\infty^{S,R}(x,z)$ are defined by Eqs. (9), the vertical structure of the modes (n=1,2,3…) is given by

$$Z_n^{(1)}(z) = \cos\left(k_n^{(1)}(z+h)\right) / \cos\left(k_n^{(1)} h\right) \ , \tag{12}$$

and the infinite set of numbers $\left\{k_n^{(1)},\ n = 1,2,..\right\}$ is obtained as the roots of the dispersion relation

$$K = -g \tan(kh), \quad K = \omega^2 / g \ . \tag{13}$$

<u>Region 3 ($0<x<b$)</u>

The general representations of the velocity potentials $\phi^{S,R}$ in the finite subdomain D_3 (interior of OWC) are

$$\phi_{(3)}^{S,R}(x,z) = \frac{f^{S,R}}{K} + C_0^{S,R} \cos\left(k_0^{(3)} x\right) Z_n^{(3)}(z) + \sum_{n=1}^{\infty} C_n^{S,R} \cosh\left(k_n^{(3)} x\right) Z_n^{(3)}(z) \quad , \tag{14}$$

where $k_n^{(3)} = k_n^{(1)}$, $n = 0,1,2,..$, and $Z_n^{(3)}(z) = Z_n^{(1)}(z)$.

The representation (14) automatically fulfills the solid boundary condition on the OWC vertical wall at x=0.

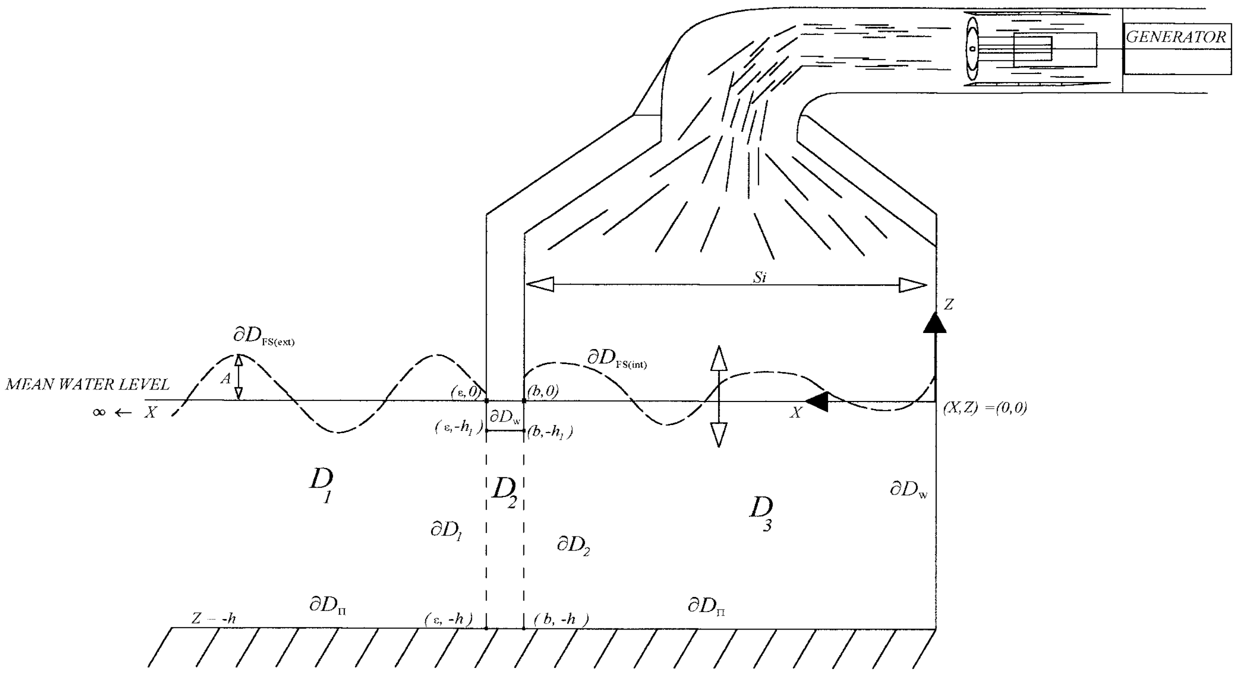

Fig. 3: Domain decomposition and basic notation

Region 2 ($b<x<\varepsilon$)

Finaly, the general representations of the velocity potentials $\phi^{S,R}$ in the finite subdomain D_2 (below the front wall of the OWC) are written as follows

$$\phi_{(2)}^{S,R}(x,z) = \left(B_{01}^{S,R}x + B_{02}^{S,R}\right)Z_0^{(2)}(z) + \sum_{n=1}^{\infty}\left(B_{n1}^{S,R}\exp\left(-k_n^{(2)}(x-b)\right) + B_{n2}^{S,R}\exp\left(k_n^{(2)}(x-\varepsilon)\right)\right)Z_n^{(2)}(z)\,. \tag{15}$$

The numbers $\left\{k_n^{(2)}, n=1,2,..\right\}$ and the functions $\left\{Z_n^{(2)}(z), n=0,1,2...\right\}$ appearing in the above expansion are given as the eigenvalues and eigenfunctions, respectively, of vertical Sturm-Liouville problems formulated in the interval $-h<z<-h_1$, satisfying Neumann boundary conditions at both ends ($z=-h$ and $z=-h_1$). These are given by

$$k_n^{(2)} = \frac{n\pi}{h-h_1}, \qquad n=1,2,3,.. , \tag{16}$$

$$Z_0^{(2)}(z) = \frac{1}{\sqrt{h-h_1}}, \qquad \text{and} \tag{17a}$$

$$Z_n^{(2)}(z) = \sqrt{\frac{2\cos 2(k_n^{(2)}h)}{h-h_1}}\;\frac{\cos\left(k_n^{(2)}(z+h)\right)}{\cos(k_n^{(2)}h)}\,. \tag{17b}$$

The solution of the hydrodynamic scattering and radiation problems is finally obtained by calculating the unknown complex coefficients $A_n^{S,R}, B_n^{S,R}, C_n^{S,R}, n=0,1,2,....$, appearing in the expansions (11), (15) and (13) in the subdomains D_1, D_2, D_3, respectively. The latter are determined by means of the matching conditions, requiring continuity of the wave potential (or equivalently the wave pressure) on the vertical interfaces separating the three subdomains:

$$\phi_{(i)}^{S,R}(x,z) = \phi_{(i+1)}^{S,R}(x,z), \quad \text{on } -h<z<-h_1,\ at\ x=\varepsilon \text{ and } x=b\,, \tag{18}$$

i=1,2, and also continuity of the horizontal velocity

$$\frac{\partial\phi_{(i)}^{S,R}(x,z)}{\partial x} = \frac{\partial\phi_{(i+1)}^{S,R}(x,z)}{\partial x}, \quad \text{on } -h<z<-h_1,\ at\ x=\varepsilon \text{ and } x=b\,, \tag{19}$$

in conjunction with the boundary conditions on the vertical solid walls of the OWC at $x=\varepsilon$ and $x=b$:

$$\frac{\partial\phi_{(i)}^{S,R}(x,z)}{\partial x} = \frac{\partial\phi_{(i+1)}^{S,R}(x,z)}{\partial x} = 0, \quad \text{on } -h_1<z<0,\ at\ x=\varepsilon \text{ and } x=b\,, \tag{20}$$

i=1,2. The final coupled-mode system for the unknown coefficients is obtained by: (i) projecting Eqs. (19), which hold in the interval $-h<z<-h_1$, to the vertical basis $Z_n^{(2)}(z), n=0,1,2....$ (defined by Eq. 17), and (ii) combining Eqs. (19) and (20), in the two parts of the vertical interval $-h<z<0$, and projecting to the corresponding vertical basis $Z_n^{(3)}(z)=Z_n^{(1)}(z), n=0,1,2....$ (defined by Eqs. 10b and 12).

As an example of the present approach, we present in Figs. 4 and 5 the calculated scattering and radiation potentials, respectively, for incident and radiated wave frequency ω=1.256 rad/s, corresponding to wave period T=5sec. In this example, the geometrical parameters associated with the length of the OWC and the depth are: b=h=10m, the front wall draft is taken $h_1=3$m and its thickness $\varepsilon-b=0.5$m .

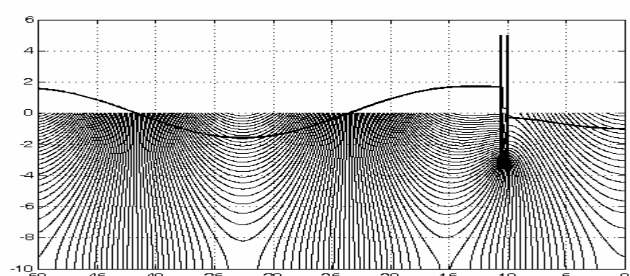

Fig. 4: Real part of scattering wave potential around the OWC device for incident waves of period T=5sec. The values of the potential on

z=0 (proportional to the upper surface elevation) are shown by using a thick solid line.

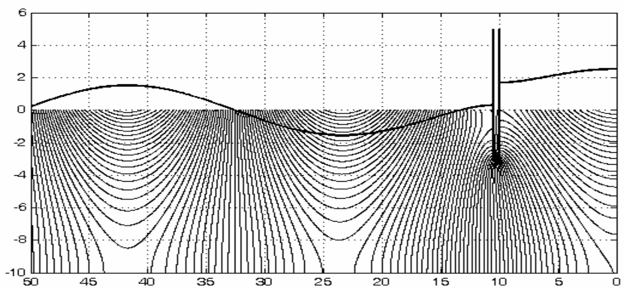

Fig. 5: Same as in Fig. 4 but for the radiation potential.

The calculations are based on truncating the modal series (11), (14) and (15) and the final coupled-mode system, by retaining 14 totally terms (modes), which was found to be enough for numerical convergence.

In Figs. 4 and 5 the wave field is shown by using equipotential lines. We are able to observe the perfect matching at the vertical interfaces, as well as the satisfaction of the Neumann boundary conditions on every solid boundary, which is equivalent to the fact that the equipotential lines intersect the solid wall perpendicularly. Also, in these figures, the values of the scattering and radiation wave potentials on the upper water surface are plotted, which are proportional to the upper surface elevation on both the exterior and interior parts of the OWC.

THERMODYNAMIC MODELING

The thermodynamic modeling of the OWC wave energy device was based on the principles of open system thermodynamic theory. The air inside the chamber is assumed to be homogeneous and the thermodynamic processes are assumed to be slow. In addition, any possible spray effects (due to wave breaking in the OWC chamber) have been neglected, and thus the homogeneity of the air in the chamber is maintained.

With only one exception, Falcao & Justino (1999), no previous derivation of the equations that govern the OWC operation was found to be illustrative enough to apply it directly. Therefore, two different approaches have been followed for the thermodynamic modeling in order to obtain a first validation test. According to the first approach, the operation of the system is described by two thermodynamic phases, whilst according to the second method by a single one.

Before we elaborate on the analysis it must be noticed that the wave elevation inside the chamber is simulated as a rigid piston, oscillating harmonically around the undisturbed upper water surface, with amplitude h_0 and frequency ω.

Description of the two approaches

During the first phase the system is considered to be closed and no air escapes or enters the chamber. Therefore, the air mass inside the chamber is constant while the volume changes as the piston (upper water surface) elevates or descends. During the second phase air enters or leaves through the turbine, which is here simply simulated as a valve, while no change in chamber's volume occurs as piston maintains its, until this phase is completed. In the second method, air mass and volume change simultaneously as the turbine inlet is always open, regardless of the position of the piston .

As far as the nature of the process is concerned no assumptions were made, e.g. adiabatic, although a relative option is available in the routine that calculates the thermodynamic quantities.

According to Gyftopoulos & Beretta (1991), the full equations describing an open thermodynamic system are presented through Eqs (21-23) below:

$$\frac{dm}{dt} = \sum_q \dot{m}_q^{\leftarrow} \ , \tag{21}$$

$$\frac{dE}{dt} = -\dot{W}_S^{\rightarrow} - p_0 \dot{V} + \dot{Q}_o^{\leftarrow} + \sum_k \dot{Q}_k^{\leftarrow} + \sum_q \dot{m}_q^{\leftarrow}\left(h_q + \frac{C_q^2}{2} + g z_q \right), \tag{22}$$

where, $\dot{m}_q^{\leftarrow}\dfrac{C_q^2}{2}$ και $\dot{m}_q^{\leftarrow} g z_q$ are rates of kinetic and dynamic energy, respectively, for an arbitrary port q (entry or exit point of mass, q=1,2,3…). Also,

$$\frac{dS}{dt} = \frac{\dot{Q}_o^{\leftarrow}}{T_o} + \sum_k \frac{\dot{Q}_k^{\leftarrow}}{T_k} + \sum_q \dot{m}_q^{\leftarrow} s_q + S_{irr} \ , \tag{23}$$

where, S_{irr} denotes the rate of the entropy production due to the irreversibility of the processes that may take place inside the system.

The equation of energy conservation adjusted to the wave energy device, see Fig.1, takes the following form

$$-p(t)\dot{V} - \dot{m}_1^{\leftarrow} h_1 + Q_{water} = \frac{dU}{dt} \Rightarrow$$

$$p(t)\dot{V} + \dot{m}_1^{\leftarrow}(h_1 - u) + \dot{m}_2^{\leftarrow}(h_2 - u) + m\frac{\partial u}{\partial t} - Q_{water} = 0 \ , \tag{24}$$

where $p(t)$ is the dynamic pressure inside the chamber of the device, h_1, h_2 are the enthalpy states at the corresponding exits, and $\dot{m}_1^{\leftarrow}, \dot{m}_2^{\leftarrow}$ are the associated mass flows (with positive sign for when air leaves the chamber). It stressed here, that exit 1 leads to a flow controlling valve, which at this stage is selected to replace the air turbine, whilst exit 2 is an additional pressure controlling valve, which in the present analysis is selected to be closed, i.e. $\dot{m}_2^{\leftarrow} = 0$. The equation describing the flow of a perfect gas through an orifice is

$$\dot{m} = C_d A_o f\left(P_u, T_u, \frac{P_d}{P_u} \right), \tag{25}$$

where $\dot{m}$ is the mass flow rate, C_d is an orifice discharging constant, A_o is the area of the orifice, T_u, P_u are the upstream pressure and temperature, respectively, and P_d is the downstream pressure.

When $\dfrac{P_d}{P_u} > \left(\dfrac{P_d}{P_u}\right)_{critical} = 0.528$ (as it always happens to be in our case), the function f in the right hand side of Eq. (25) becomes

$$f\left(P_u, T_u, \frac{P_d}{P_u} \right) = \frac{W}{C_d A_o} = 2.06 \frac{P_u}{\sqrt{T_u}} \left(\frac{P_d}{P_u} \right)^{1-\gamma} \sqrt{1 - \left(\frac{P_d}{P_u} \right)^{(\gamma-1)/\gamma}} \ . \tag{26}$$

Converting the above into the S.I. unit system and using it in Eq. (25), the latter becomes:

$$\dot{m} = C_V A_{Veq} \frac{P_u}{\sqrt{RT_u}} \sqrt{\left(\frac{2\gamma}{\gamma-1}\right)\left\{\left(\frac{P_d}{P_u}\right)^{2/\gamma} 1 - \left(\frac{P_d}{P_u}\right)^{(\gamma+1)/\gamma}\right\}} \,, \tag{27}$$

where $C_V = 0.9$, and $A_{Veq} = 0.75m^2$.

The air volume inside the OWC at each time t is given by

$$V = V_{OWC} - V_{Piston} = V_{OWC} - Area \cdot h_o \cdot \cos(\omega t) \,. \tag{28}$$

Having obtained the above differential equations that depict the dynamics of the OWC thermal subsystem, integration in order to obtain a solution has to be performed by some scheme. As already mentioned, two approaches have been followed in this work for cross-reference purposes. In both methods, however, the initial values for the air pressure and temperature inside the OWC chamber are set equal to the atmospheric ones. Furthermore, the air mass is calculated as the product of the air density at atmospheric conditions times the volume of the chamber when the upper water surface is at rest. For simplicity, the OWC air chamber has been assumed to be orthogonal box-shaped with volume $V(t=0) = V_{OWC}$.

According to the first method, there are two elementary thermodynamic stages to be performed at each time step. The first step is a closed-system compression or expansion (closed in this context means that through the valve representing the turbine air flow rate is set to zero) followed by a constant volume air discharge or intake.

In order to introduce heat transfer, heat flow through the air-water interface is assumed. The heat flow rate then is calculated as follows:

$$\dot{Q}_c = -g_{th}(T_{initial} - T_{water}) \Rightarrow dQ_c = \dot{Q}_c \, dt \Rightarrow dq_c = dQ_c / m_c \tag{29}$$

where the thermal conductivity g_{th} is taken to be $g_{th} = 10S_i$ W/degK.

From the first thermodynamic law one may obtain the following relations

$$du = dq - Pd\hat{v} \Rightarrow c_v dT = dq - Pd\hat{v} \text{ where } \frac{d\hat{v}}{\hat{v}} = \frac{dV}{V_{initial}} - \frac{dm}{m_{initial}} \,.$$

Thus,

$$dT = \frac{dq}{c_v} - \frac{P_{initial}}{c_v}\left(\frac{dV}{V_{initial}} - \frac{dm}{m_{initial}}\right) \,, \tag{30}$$

During this stage the system is closed $dm = 0$ and thus,

$$dT = \frac{dq}{c_v} - \frac{P_{initial}}{c_v}\frac{dV}{V_{initial}} \,. \tag{31}$$

Consequently, we obtain $T_{closed_{final}} = T_{closed_{initial}} + dT$. From the ideal gas law the air pressure at the first stage is calculated as follows:

$$P_{closed} = \frac{m_{initial} R T_{closed_{final}}}{V_{closed_{final}}} \,. \tag{32}$$

During the second stage of the first integration method, the initial values of temperature and pressure will be set equal to the corresponding final values of the first stage while the air volume is equal to the volume after the completion of the compression or decompression performed at the first stage. A point, needing attention before the calculations of this stage are performed, is to check whether in-chamber pressure is higher or lower than the atmospheric one. According to the result air either enters or exits the chamber. Correspondingly, the chamber acts either as upstream or downstream for air flow. In effect, Eq. (27) for air mass flow rate is adjusted accordingly.

An additional amount of heat is also passed to the water through the air-water interface, during this stage as well. It can be calculated as previously: (7)

$$\dot{Q}_{open} = -g_{th}(T_{closed_{final}} - T_{water}) \Rightarrow dQ_{open} = \dot{Q}_{open} \, dt \Rightarrow$$
$$dq_{open} = dQ_{open} / m_{closed}$$

The first law of thermodynamics yields:

$$du = dq - Pd\hat{v} \Rightarrow c_v dT = dq - Pd\hat{v} \,, \quad \text{where} \quad \frac{d\hat{v}}{\hat{v}} = \frac{dV}{V_{closed_{final}}} - \frac{dm}{m_{initial}} \,.$$

Thus:

$$dT_{open} = \frac{dq}{c_v} - \frac{P_{closed_{final}}}{c_v}\left(\frac{dV}{V_{closed_{final}}} - \frac{dm}{m_{initial}}\right) . \tag{33}$$

During this phase the chamber is open, i.e. $dm \neq 0$, but the piston does not move and consequently the volume remains constant, i.e. $dV = 0$. Thus, the temperature difference is given by:

$$dT_{open} = \frac{dq}{c_v} + \frac{P_{closed_{final}}}{c_v}\frac{dm}{m_{initial}} \,. \tag{34}$$

After both stages the temperature and mass inside the OWC chamber are calculated as follows:

$$T_{final} = T_{closed_{final}} + dT_{open} \,, \tag{35}$$

$$m_{final} = m_{initial} + dm_{open} \,. \tag{36}$$

Finally, from the ideal gas law the the air pressure after both stages is obtained, as follows

$$P_{final} = \frac{m_{final} R T_{final}}{V} \,,. \tag{37}$$

According to the second integration approach, each time step corresponds to a single stage but for a thermodynamic system considered to be open. As heat transfer from the air to the water through the interface is assumed, the elementary amount of heat transferred is calculated as follows:

$$\begin{aligned} &\dot{Q} = -g_{th}(T_{initial} - T_{water}) \Rightarrow \\ &dQ = \dot{Q}\, dt \Rightarrow dq = dQ / m_{initial} \end{aligned} \tag{38}$$

Again, the air pressure value must be checked if it is higher or lower than the atmospheric one prior of performing the elementary mass transfer. Then, by using Eq. (27) it is obtained:

$$dm = \dot{m}\, dt \tag{39}$$

$$m_{final} = m_{initial} + dm \tag{40}$$

Applying the first law of thermodynamics, the temperature difference is calculated. Consequently, the air temperature inside the chamber is given by:

$$dT = \frac{dq}{c_v} - \frac{P_{initial}}{c_v}\left(\frac{dV}{V_{initial}} - \frac{dm}{m_{initial}}\right), \tag{41}$$

$$T_{final} = T_{initial} + dT \,. \tag{42}$$

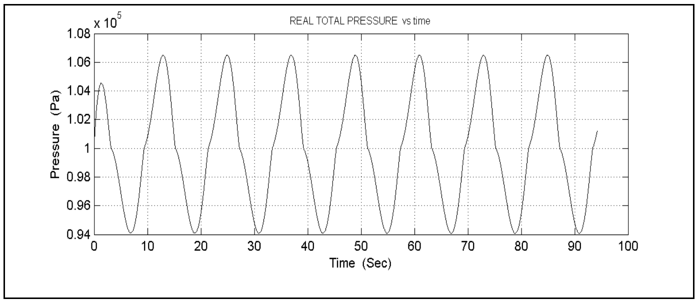

Fig. 6: Absolute in-chamber air pressure for monochromatic piston motion of frequency 0.1Hz. The volume swept by the piston (peak-to-peak) is 280 m^3.

Finally, by the ideal gas law the air pressure at the time step end is:

$$P_{final} = \frac{m_{final} R T_{final}}{V_{final}} \quad . \tag{43}$$

By implementing both integration approaches in Matlab©, it has been seen that both they provide identical results, for all state variables of the thermodynamic subsystem. For a period T=10sec, typical results by using the single-stage model for sinusoidal piston motion are shown in Fig. 6, for the geometrical configuration of Fig. 4 and piston motion corresponding to 280m^3 volume swept by the piston.

SYSTEM IDENTIFICATION

As stated in the introduction, for the nonlinear thermodynamic part a Volterra approach is adopted leading to a truncated polynomial representation. The corresponding analysis can be found in Rugh (1981) as well as in Xiros and Georgiou (2005). However, this method provides satisfactory results only for narrow ranges of frequencies and amplitudes. Therefore, instead of a single model for the entire band and amplitude range of interest, a family of models parameterized by the excitation amplitude and frequency was obtained. Here it is noted that these models concern only monochromatic inputs. The structure of the all the models of the family was chosen to be the one proposed by Rugh (1981). As can be seen in Fig. 7 it is a polynomial system.

The polynomial coefficients a_1, a_2, a_3 are depended on the amplitude, A^*, and the frequency ω_{ref} of the excitation, as follows:

$$a_1 = a_1(A^*, \omega_{ref}), a_2 = a_2(A^*, \omega_{ref}), a_3 = a_3(A^*, \omega_{ref}) \tag{44}$$

The linear filters of the model obtain impulse responses G_1, G_2 parameterized by the excitation frequency, i.e.:

$$g_1(t;\omega_{ref}), g_2(t;\omega_{ref}) \ . \tag{45}$$

In the relationships above the reference frequency ω_{ref} is evidently a function of the excitation frequency ω_{exc}. In specific, the frequency band of interest has been partitioned to sub-bands around the central frequencies ω_{ref}. Thus, the identification of our thermodynamic part of an OWC installation is as shown in Fig.7.

The response of the model f or sinusoidal excitation of the form

$u(t) = 2A^* \cos(\omega_{exc} t)$ is a sum of three harmonics as follows:

$$\begin{aligned} y(t) &= Y_0 + Y_1\left(A^*, \omega_{ref}(\omega_{exc})\right)\cos\left(\omega_{exc} t + \theta_1\right) + \\ &+ Y_2\left(A^*, \omega_{ref}(\omega_{exc})\right)\cos\left(2\omega_{exc} t + \theta_2\right) + \\ &+ Y_3\left(A^*, \omega_{ref}(\omega_{exc})\right)\cos\left(3\omega_{exc} t + \theta_3\right) \end{aligned} \tag{46}$$

By matching the amplitude of the response's first harmonic to that of the air pressure response to identical sinusoidal water level excitation, it is possible to obtain the values of the model parameters as shown in Rugh (1981) and Xiros and Georgiou (2005). This is achieved through a Least-Squares procedure carried out entirely in the frequency domain. The advantage of the proposed method is that it employs only the power of the first harmonic for the identification of all nonlinear model parameters. However, it must be verified beforehand that the response of the process to be identified obtains a spectrum structure compatible to the order of the static polynomial nonlinearity intermitted between the linear filters. Otherwise, the choice of a polynomial model may not be adequate.

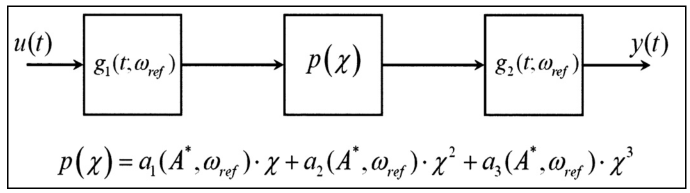

Fig. 7: Structure of the nonlinear polynomial model for identification.

Nevertheless, in our case as seen in Fig. 8, the third-order polynomial model adequately reproduces the spectrum structure of the thermodynamic subsystem's response, since no significant peaks appear in harmonics higher than 3 in all cases examined. Another remark which can be directly derived from the governing principles, as well, is the lack of zero-frequency (DC) component in the thermodynamic response. This is deduced from the fact that when the spatially-averaged, in-chamber water lever is constant, the pressure remains equal to its equilibrium value. Alternatively, when the thermodynamic system was driven by initial values only (i.e. an initial value of pressure and/or temperature other than the atmospheric ones) it finally converged to the atmospheric values for all thermodynamic state variables.

CONCLUSIONS

In this work a new model is developed for the dynamics of Oscillating Water Column (OWC) wave energy extraction systems, based on system identification techniques. The wave field is modeled on the basis of linear water wave theory, while for the air entrapped inside the OWC an open thermodynamic system approach has been employed. Following previous works, the wave field outside the OWC is expressed as superposition of the scattering and radiation potentials, the latter being formulated per unit dynamic pressure in the OWC chamber. As concerns the thermodynamic part of the system, Volterra-theory techniques have been employed, providing us with an input-output, black-box, nonlinear model describing the dynamics of the entrapped air pressure responses to monochromatic oscillations of the mean water level inside the OWC at various frequencies. This input-output description of the thermodynamic part can be used, in conjunction to the hydrodynamic model, for the investigation of the termination conditions imposed to the wave field by the OWC device. Future work is directed towards the application of the present model to studies aiming to analyze and improve the overall efficiency of the installation. Furthermore, the present model will be combined with the consistent coupled-mode model developed by Athanassoulis & Belibassakis (1999), for the propagation of water waves in variable bathymetry, in order to estimate the effects of variable bottom topography to the operation and control of the OWC installed at realistic nearshore/coastal sites.

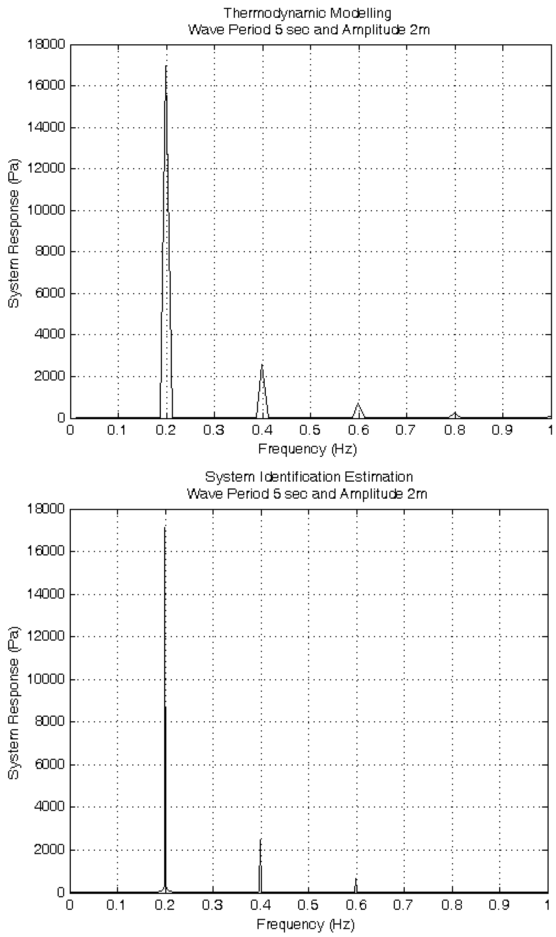

Fig. 8: Frequency-domain comparison of sinusoidal response of the thermodynamic numerical code (top) to that of the Volterra polynomial model (bottom), for *T*=5sec.

ACKNOWLEDGEMENTS
George Gkikas wishes to acknowledge the Greek State Scholarships Foundation (IKY) for financially supporting his postgraduate studies.

REFERENCES

Athanassoulis, G.A., Belibassakis, K.A. (1999) “A consistent coupled-mode theory for the propagation of small-amplitude water waves over variable bathymetry regions”, *J. Fluid Mech*., Vol. 389, 275-301.

Black, JL, and Mei CC, and Bray, MCG (1971), "Radiation and scattering of water waves by rigid bodies", *J Fluid Mech*, Vol 46, pp 151-164.

Evans, DV, and Porter, R (1995), "Hydrodynamic characteristics of an oscillating water column device", *Applied Ocean Research*, Vol 17, pp155-164.

Evans, DV (1982), "Wave Power Absorption by Systems of Oscillating Surface Pressure Distributions", *J Fluid Mech,* Vol 114, pp 481-499.

Evans, DV (1978), "The Oscillating Water Column wave energy device", *J Inst Maths Applics*, Vol 22, pp 423-33.

Falcão, AF de O (2001), "Wave-power absorption by a periodic linear array of oscillating water columns", *Ocean Engineering,* Vol 29, No 10, pp 1163-1186.

Falcão, AF de O (2002), "Control of an oscillating-water-column wave power plant for maximum energy production", *Applied Ocean Research*, Vol 24, 73-82.

Falcão, AF de O, and Justino, PAP (1999), "OWC wave energy devices with air flow control", *Ocean Engineering*, Vol 26, No 12, pp1275-1295

Falcão, AF de O, and Rodrigues, JA (2002), "Stochastic modelling of OWC wave power plant performance", *Applied Ocean Research*, Vol 24, No 2, pp 59-71.

Falnes, J (2002), "*Ocean Waves and Oscillating Systems-Linear Interactions Including Wave-Energy Extraction*", Department of Physics, Norwegian University of Science and Technology NTNU, Cambridge University Press.

Falnes, J, and McIver, P (1985), "Surface Wave Interactions with Systems of Oscillating Bodies and Pressure Distributions", *Applied Ocean Research*, Vol 7, pp 225-34.

Gyftopoulos, P, and Beretta, GP (1991), "Thermodynamics: Foundations & Applications", McMillan.

Kestin, J (1996), "*A course in Thermodynamics*", Blaisdel, Waltham, MA.

Mei, CC (1983), "*The applied Dynamics of Ocean Surface Waves*", John Wiely & Sons, Wiely-Interscience Publications, New York.

Mei, CC, and Black, JL (1969), "Scattering of surface waves by rectangular obstacles in water of finite depth", *J Fluid Mech*, Vol 33, pp 499-511.

Porter, R, and Evans, DV (1995), "Complementary Approximations to Wave Scattering by Vertical Barriers", *J Fluid Mech*, Vol 294, pp 155-80.

Rugh, WJ (1981) “*Nonlinear system theory; the Voltera/Wiener approach*”, J.Hopkins Univ. Press.

Thiruvenkatasamy, K, and Neelamani, S (1997). "On the efficiency of wave energy caissons in array", *Applied Ocean Research*, Vol 19, pp 61 - 72.

Xiros, NI, and Georgiou, IT (2005) “Analysis of coupled electromechanical oscillators by a band-pass, reduced complexity, Volterra method”, 2005 ASME IMECE, Orlando, Florida.

Wehausen, JV, and Laitone, EV (1960), "Surface Waves", *Encyclopedia of Physics*, Vol 9 / III, Springer-Verlag.